Synthesis and Structural Characterization of the New *hypho*-Carborane Clusters *endo*-7-[Ph_2(H)P]-8-R-*hypho*-7,8-$C_2B_6H_{11}$ with Ylide-Like Cage Carbons

Daewon Hong, Patrick J. Carroll, and Larry G. Sneddon*

Department of Chemistry, University of Pennsylvania, Philadelphia, Pennsylvania 19104-6323

Received November 1, 2003

The new hypho-class carboranes *endo*-7-[Ph_2(H)P]-8-R-*hypho*-7,8-$C_2B_6H_{11}$ (R = H, Me) were prepared from the reactions of Na^+[*arachno*-4,6-$C_2B_7H_{12}$]$^-$ and Na^+[4-Me-*arachno*-4,6-$C_2B_7H_{11}$]$^-$ with Ph_2PCl. Single-crystal X-ray crystallographic determinations and DFT/GIAO computational studies established that while the *endo*-7-[Ph_2(H)P]-8-R-*hypho*-7,8-$C_2B_6H_{11}$ cages (R = H, Me) have frameworks that are consistent with those which have been adopted by other isoelectronic eight-vertex hypho clusters, the cage carbon having the Ph_2(H)P substituent exhibits a shortened phosphorus−carbon bond, suggesting an ylide-like character.

Introduction

As the number of skeletal electrons of an electron-deficient cluster is increased, the cage normally responds by adopting more and more open structures until eventually an electron-precise "classical" structure is achieved. However, in many cases, rather than affecting the entire cage structure, the addition of electrons to a cage may result in a conversion of a portion of the cage framework to an apparently "classical" fragment, with the remainder of the structure unchanged. In this paper, the syntheses and structural characterizations of two new phosphine-substituted carboranes are described. The structures of these compounds can be alternately viewed as R_2PH-substituted, eight-vertex, hypho clusters, i.e., *endo*-7-[Ph_2(H)P]-8-R-*hypho*-7,8-$C_2B_6H_{11}$ (R = H, Me), or seven-vertex arachno clusters that are bonded to a "classical" phosphorus ylide fragment, i.e., $\mu_{2,6}$-[Ph_2(H)P═C(H)]-8-R-*arachno*-8-CB_6H_{10}.

Experimental Section

All manipulations were carried out using standard high-vacuum or inert-atmosphere techniques as described by Shriver.[1]

Materials. Iodomethane and chlorodiphenylphosphine were purchased from Aldrich and used as received. Oil-dispersed NaH was purchased from Aldrich, washed with dry hexanes under a N_2 atmosphere, and dried under high vacuum prior to use. 1,2-Dimethoxyethane (DME), dichloromethane (DCM), and hexanes (Hex) were dried by passing through an activated alumina column prior to use. *arachno*-4,6-$C_2B_7H_{13}$ was prepared according to literature procedures.[2]

Physical Measurements. ^{1}H NMR spectra at 500.4 MHz, ^{11}B NMR spectra at 160.5 MHz, and ^{13}C NMR at 125.8 MHz were obtained on a Bruker AM-500 spectrometer equipped with the appropriate decoupling accessories. The ^{31}P NMR spectra at 145.8 MHz were obtained on a Bruker AM-360 spectrometer. All ^{11}B chemical shifts are referenced to external BF_3·OEt_2 (0.00 ppm), with a negative sign indicating an upfield shift. The ^{1}H and ^{13}C chemical shifts were measured relative to internal residual protons or carbons in the lock solvent and are referenced to Me_4Si (0.00 ppm). All ^{31}P chemical shifts are referenced to external 85% H_3PO_4 (0.00 ppm), with a negative sign indicating an upfield shift. The melting points were obtained on a standard melting point apparatus and are uncorrected. High-resolution mass spectra were obtained on a Micromass Autospec mass spectrometer. Elemental analyses were performed at the University of Pennsylvania microanalysis facility. Infrared spectra were obtained on a Perkin-Elmer 1430 spectrophotometer.

***endo*-7-[Ph_2(H)P]-*hypho*-7,8-$C_2B_6H_{12}$ (1).** A 0.115 g (1.0 mmol) sample of *arachno*-4,6-$C_2B_7H_{13}$ was dissolved in 10 mL of DME. Excess NaH (∼0.1 g, ∼4 mmol) was then added at 0 °C. After Na^+[*arachno*-4,6-$C_2B_7H_{12}$]$^-$ was observed to have formed by ^{11}B NMR analysis, the reaction mixture was filtered to remove excess NaH. The Na^+[*arachno*-4,6-$C_2B_7H_{12}$]$^-$ DME solution was maintained at 0 °C, while 0.24 mL (1.3 mmol) of Ph_2PCl was slowly added. The mixture was brought to room temperature and stirred for 15 h, at which point ^{11}B NMR analysis showed the formation of **1**. The mixture was filtered, and the volatiles were removed from the filtrate in vacuo. The crude product was purified by preparative TLC using Hex/DCM cosolvent (1:1, v/v) to give 0.084 g (0.29 mmol, 29%) of white solid **1**, mp 146−148 °C dec. Anal. Calcd: C, 58.29; H, 8.04. Found: C, 57.90; H, 8.12. HRMS (*m*/*e*): calcd for $^{12}C_{14}{}^1H_{23}{}^{11}B_6{}^{31}P$, 288.2103; found, 288.2100. IR (CH_2Cl_2, NaCl, cm^{-1}): 2500 (s), 1440 (m), 1110 (m), 1060 (m), 950 (m), 900 (m).

***endo*-7-[Ph_2(H)P]-8-Me-*hypho*-7,8-$C_2B_6H_{11}$ (2).** A 0.122 g (1.1 mmol) sample of *arachno*-4,6-$C_2B_7H_{13}$ was dissolved in 5 mL of DME. Excess NaH (∼0.1 g, ∼4 mmol) was then added at 0 °C. After Na^+[*arachno*-4,6-$C_2B_7H_{12}$]$^-$ was formed, the reaction mixture was filtered to remove excess NaH. Excess iodomethane (0.3 mL, 5 mmol) was next added to the filtrate under argon. The reaction progress was monitored by ^{11}B NMR analysis. If necessary, additional NaH and iodomethane were alternately introduced until the reaction was complete.[3] The solvent and residual iodomethane were removed in vacuo to

(1) Shriver, D. F.; Drezdzon, M. A. *Manipulation of Air-Sensitive Compounds*, 2nd ed.; Wiley: New York, 1986.
(2) Garrett, P. M.; George, T. A.; Hawthorne, M. F. *Inorg. Chem.* **1969**, *8*, 2008−2009.

10.1021/om034274h CCC: $27.50
Publication on Web 01/15/2004

Table 1. Crystallographic Data and Data Collection and Structure Refinement Details

	1	**2**
empirical formula	$C_{14}B_6H_{24}P$	$C_{15}B_6H_{25}P$
formula wt	288.16	301.18
cryst class	orthorhombic	monoclinic
space group	$P2_12_12_1$	$P2_1/n$
Z	8	4
a, Å	10.199(2)	8.9973(3)
b, Å	16.768(3)	10.9389(2)
c, Å	19.803(3)	18.3373(6)
β, deg		93.687(1)
V, Å^3	3386.6(9)	1801.03(9)
μ, cm^{-1}	1.48	1.42
cryst size, mm	0.38 × 0.34 × 0.30	0.48 × 0.10 × 0.07
D_{calcd}, g/cm^3	1.130	1.111
$F(000)$	1224	640
radiation	Mo Kα (λ = 0.710 69 Å)	Mo Kα (λ = 0.710 69 Å)
2θ angle, deg	5.1−54.96	5.18−50.68
hkl collected	$-13 \le h \le 13$, $-17 \le k \le 21$, $-24 \le l \le 25$	$-10 \le h \le 9$, $-13 \le k \le 13$, $-22 \le l \le 22$
no. of rflns measd	23 173	13 529
no. of unique rflns	7503 (R_{int} = 0.0417)	3250 (R_{int} = 0.0565)
no. of obsd rflns	6526 ($F > 4\sigma$)	2945 ($F > 4\sigma$)
no. of rflns used in refinement	7503	3250
no. of params	483	248
R^a indices ($F > 4\sigma$)	R1 = 0.0606	R1 = 0.0646
	wR2 = 0.1462	wR2 = 0.1264
R^a indices (all data)	R1 = 0.0707	R1 = 0.0734
	wR2 = 0.1519	wR2 = 0.1303
GOF[b]	1.051	1.194
final diff peaks, e/Å^3	+0.488, −0.245	+0.223, −0.375

[a] $R1 = \sum||F_o| - |F_c||/\sum|F_o|$; $wR2 = \{\sum w(F_o^2 - F_c^2)^2/\sum w(F_o^2)^2\}^{1/2}$. [b] $GOF = \{\sum w(F_o^2 - F_c^2)^2/(n-p)\}^{1/2}$ where n = no. of reflections and p = no. of parameters refined.

give solid Na$^+$[4-Me-*arachno*-4,6-$C_2B_7H_{11}$]$^-$, which was then redissolved in 7 mL of DME. The reaction mixture was maintained at 0 °C, while 0.22 mL (1.1 mmol) of Ph_2PCl was slowly added. The mixture was brought to room temperature and stirred for 5 h, at which point ^{11}B NMR analysis showed the formation of **2**. The mixture was then filtered, and the volatiles were removed from the filtrate in vacuo. The crude product was purified by preparative TLC using Hex/DCM cosolvent (1:1, v/v) to give 0.126 g (0.42 mmol, 38%) of white solid **2**, mp 59 °C dec. Anal. Calcd: C, 59.56; H, 8.34. Found: C, 59.44; H, 7.59. HRMS (*m*/*e*) calcd for $^{12}C_{15}{}^1H_{25}{}^{11}B_6{}^{31}P$ 302.2252, found 302.2244. IR (CH_2Cl_2, NaCl, cm^{-1}): 2950 (m), 2880 (w), 2850 (m), 2550 (s), 2500 (s), 2450 (w), 1450 (s), 1220 (m), 1050 (m), 890 (s).

X-ray Intensity Data Collection. X-ray intensity data were collected on either Rigaku Mercury CCD (**1**, Penn #3195) or Rigaku R-AXIS IIc (for **2**, Penn #3191) area detectors employing graphite-monochromated Mo Kα radiation (λ = 0.710 69 Å) at 143 K (**1**) and 295 K (**2**). Indexing was performed from a series of 0.5° (**1**) and 1° (**2**) oscillation images with exposures of 10 (**1**) and 250 s/frame (**2**). For each compound, a hemisphere of data was collected using 0.5° (**1**) and 6° (**2**) oscillation angles, with exposures of 10 (**1**) and 500 s/frame (**2**) and crystal-to-detector distances of 35 (**1**) and 82 mm (**2**). Crystallographic data and data collection and structure refinement details are given in Table 1.

Reduction of the Data. Oscillation images were processed using bioteX,[4] producing a listing of unaveraged F^2 and $\sigma(F^2)$ values which were then passed to the teXsan[5] program package for further processing and structure solution on a Silicon Graphics Indigo R4000 computer. The intensity data were corrected for Lorentz and polarization effects, but not for absorption.

Computational Studies. The DFT/GIAO/NMR method,[6] using the Gaussian 98[7] program, was used in a manner similar to that previously described.[8] The geometries were fully optimized at the B3LYP/6-311G* level within the specified symmetry constraints (using the standard basis sets included) on a (4)-processor Origin 200 computer running IRIX 6.5.5. A vibrational frequency analysis was carried out on each optimized geometry at the B3LYP/6-311G* level with a true minimum found for each structure (i.e. possessing no imaginary frequencies). The NMR chemical shifts were calculated at the B3LYP/6-311G* level using the GIAO option within Gaussian 98. The ^{11}B NMR GIAO chemical shifts are referenced to $BF_3{\cdot}OEt_2$ using an absolute shielding constant of 102.24.[8,9] The ^{13}C NMR GIAO chemical shifts are referenced to TMS using an absolute shielding constant of 184.38.[8,9] The ^{31}P NMR GIAO chemical shifts were first referenced to PH_3 using an absolute shielding constant of 557.2396 ppm and then converted to the H_3PO_4 reference scale using the experimental value of $\delta(PH_3)$ −240 ppm.[10]

Results and Discussion

The Na$^+$[*arachno*-4,6-$C_2B_7H_{12}$]$^-$ and Na$^+$[4-Me-*arachno*-4,6-$C_2B_7H_{11}$]$^-$ salts were reacted as shown in eq 1 with Ph_2PCl to produce *endo*-7-[Ph_2(H)P]-8-R-*hypho*-7,8-$C_2B_6H_{11}$ (R = H (**1**), Me (**2**)) in 29 and 38% isolated yields, respectively.

$$\text{Na}^+[\text{4-R-}\textit{arachno}\text{-4,6-}C_2B_7H_{11}]^- + Ph_2PCl \xrightarrow{-\text{NaCl, ``B''}} \textit{endo}\text{-7-[}Ph_2\text{(H)P]-8-R-}\textit{hypho}\text{-7,8-}C_2B_6H_{11} \quad (1)$$

R = H (**1**), Me (**2**)

The compositions of the products were confirmed by elemental analyses and high-resolution mass spectrometry. Both compounds are air-stable for short periods and soluble in benzene, dichloromethane, and hexanes.

If the cage frameworks in **1** and **2** are each considered to have 8 vertexes (2 C's and 6 B's), with the Ph_2(H)P substituents functioning as two-electron donors to the cages, then the cages would contain 24 skeletal elec-

(3) Kadlecek, D. E.; Hong, D.; Carroll, P. J.; Sneddon, L. G. Manuscript in preparation.
(4) bioteX: A Suite of Programs for the Collection, Reduction and Interpretation of Imaging Plate Data; Molecular Structure Corp., The Woodlands, TX, 1995.
(5) Crystal Structure Analysis Package; Molecular Structure Corp., The Woodlands, TX, 1985, 1992.
(6) Yang, X.; Jiao, H.; Schleyer, P. v. R. *Inorg. Chem.* **1997**, *36*, 4897−4899 and references therein.
(7) Frisch, M. J.; Trucks, G. W.; Schlegel, H. B.; Scuseria, G. E.; Robb, M. A.; Cheeseman, J. R.; Zakrzewski, V. G.; Montgomery, J. A., Jr.; Stratmann, R. E.; Burant, J. C.; Dapprich, S.; Millam, J. M.; Daniels, A. D.; Kudin, K. N.; Strain, M. C.; Farkas, O.; Tomasi, J.; Barone, V.; Cossi, M.; Cammi, R.; Mennucci, B.; Pomelli, C.; Adamo, C.; Clifford, S.; Ochterski, J.; Petersson, G. A.; Ayala, P. Y.; Cui, Q.; Morokuma, K.; Malick, D. K.; Rabuck, A. D.; Raghavachari, K.; Foresman, J. B.; Cioslowski, J.; Ortiz, J. V.; Stefanov, B. B.; Liu, G.; Liashenko, A.; Piskorz, P.; Komaromi, I.; Gomperts, R.; Martin, R. L.; Fox, D. J.; Keith, T.; Al-Laham, M. A.; Peng, C. Y.; Nanayakkara, A.; Gonzalez, C.; Challacombe, M.; Gill, P. M. W.; Johnson, B. G.; Chen, W.; Wong, M. W.; Andres, J. L.; Head-Gordon, M.; Replogle, E. S.; Pople, J. A. *Gaussian 98*, revision A.9; Gaussian, Inc.: Pittsburgh, PA, 1998.
(8) (a) Keller, W.; Barnum, B. A.; Bausch, J. W.; Sneddon, L. G. *Inorg. Chem.* **1993**, *32*, 5058−5066. (b) Bausch, J. W.; Rizzo, R. C.; Sneddon, L. G.; Wille, A. E.; Williams, R. E. *Inorg. Chem.* **1996**, *35*, 131−135. (c) Tebben, A. J. Master's Thesis, Villanova University, 1997. (d) Kadlecek, D. E.; Carroll, P. J.; Sneddon, L. G. *J. Am. Chem. Soc.* **2000**, *122*, 10868−10877.
(9) Tebben, A. J.; Bausch, J. W. Private communication.
(10) Shedlow, A. M.; Sneddon, L. G. *Inorg. Chem.* **1998**, *37*, 5269−5277.

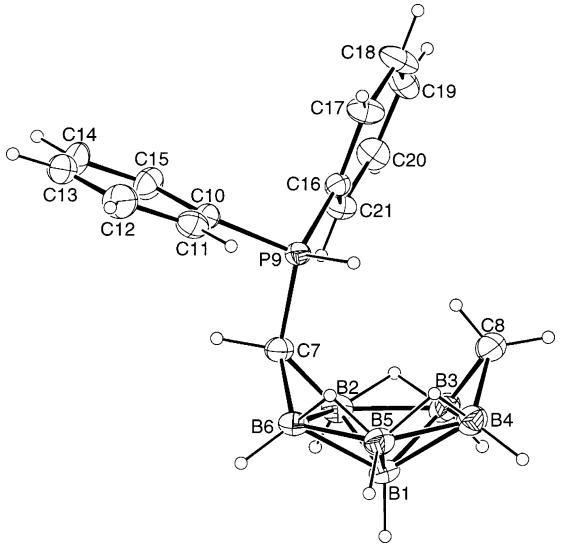

Figure 1. ORTEP drawing of *endo*-7-[Ph_2(H)P]-*hypho*-7,8-$C_2B_6H_{12}$ (**1**). Selected bond distances (Å) and angles (deg): P9−C7, 1.737(3); P9−C10, 1.781(3); P9−C16, 1.801(3); P9−H9, 1.39(3); B2−C7, 1.612(5); B6−C7, 1.618(5); B3−C8, 1.603(6); B4−C8, 1.570(6); B2−B6, 1.981(5); B2−B3, 1.795(6); B3−B4, 1.976(6); B4−B5, 1.804(6); B5−B6, 1.806(5); C7−P9−C10, 107.5(2); C7−P9−C16, 116.75(14); C10−P9−C16, 110.38(13); C7−P9−H9, 104.3(14); P9−C7−C7H, 95(2); C8Ha−C8−C8Hb, 119(3).

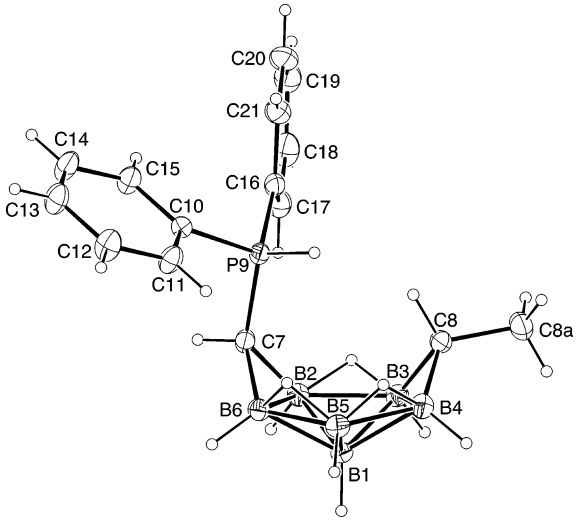

Figure 2. ORTEP drawing of *endo*-7-[Ph_2(H)P]-8-Me-*hypho*-7,8-$C_2B_6H_{11}$ (**2**). P9−C7, 1.742(3); P9−C10, 1.797(3); P9−C16, 1.795(3); P9−H9, 1.32(2); B2−C7, 1.624(4); B6−C7, 1.620(4); B3−C8, 1.587(4); B4−C8, 1.564(4); B2−B6, 1.978(4); B2−B3, 1.823(4); B3−B4, 1.962(4); B4−B5, 1.809(4); B5−B6, 1.809(4); C7−P9−C10, 108.81(12); C7−P9−C16, 114.90(13); C10−P9−C16, 107.90(12); C7−P9−H9, 111.2(10); C8a−C8−C8H, 111(2); P9−C7−C7H, 104(2).

trons.[11] Compounds of this composition should then adopt the hypho cage geometry ($n + 4$ skeletal electron pairs), based upon an octadecahedron missing 3 vertexes, that has been observed for the isoelectronic eight-vertex clusters *hypho*-$C_2B_6H_{13}^-$, *hypho*-2,3-$S_2B_6H_9^-$, 2,3-Me_2-*hypho*-2,3-$S_2B_6H_8$, *endo*-7-CH_3-*hypho*-7,8-$NC_2B_6H_{11}$, and *endo*-7-CH_3-*hypho*-7,8-$NC_2B_6H_{11}$.[12−14] Consistent with this prediction, single-crystal X-ray diffraction studies of **1** and **2** confirmed the structures shown in Figures 1 and 2. The compounds can be considered as Ph_2(H)P-substituted derivatives of the known *hypho*-$C_2B_6H_{13}^-$ anion,[12] having structures in which the two cage carbons are bonded at nonadjacent edges of the pentagonal-pyramidal boron framework.

Although **1** and **2** have the same skeletal framework as *hypho*-$C_2B_6H_{13}^-$, the synthetic route leading to **1** and **2** is very different from that used to obtain *hypho*-$C_2B_6H_{13}^-$. *hypho*-$C_2B_6H_{13}^-$ was synthesized from the reaction of the adjacent-carbon *arachno*-4,5-$C_2B_7H_{13}$ with aqueous NaCN,[12] while **1** was prepared from the nonadjacent-carbon *arachno*-4,6-$C_2B_7H_{13}$. Although the detailed mechanism of the boron loss that occurs upon the formation of **1** and **2** has not been determined, it is known that the boron atoms between the two heteroatoms in both of the isoelectronic *arachno*-4,6-$C_2B_7H_{13}$ and *arachno*-6,8-$S_2B_7H_9$ clusters are susceptible to nucleophilic attack.[13,15] Thus, it is reasonable that loss of the B5 boron between the two carbons in *arachno*-4,6-$C_2B_7H_{13}$ could be aided by phosphine attack. If this results in loss of phosphine−borane, then hydrogen transfer to the resulting C_2B_6 carborane fragment, most likely from other borane fragments formed during the reactions, must also occur to produce **1** and **2**.

In *hypho*-$C_2B_6H_{13}^-$, both cage carbons have endo hydrogens, but in **1** and **2**, one of the endo hydrogens at C7 has been replaced by the *endo*-Ph_2(H)P substituent. As found both in *hypho*-$C_2B_6H_{13}^-$ and *hypho*-2,3-$S_2B_6H_9^-$, bridge hydrogens are present at the B2−B3, B4−B5, and B5−B6 edges in **1** and **2**.

The NMR spectroscopic data (Table 2) are consistent with the crystallographically determined structures, as well as for the DFT/GIAO calculated (B3LYP/6-311G*) ^{11}B, ^{31}P, and ^{13}C chemical shifts for the optimized geometries (B3LYP/6-311G*) **I** (for **1**) and **II** (for **2**) shown in Figure 3. Thus, in their ^{11}B NMR spectra, **1** and **2** show a six-resonance pattern consistent with the established C_1 cage symmetry, with both the chemical shift values and assignments matching the calculated values. Likewise, the ^{31}P NMR spectra of these compounds show doublet resonances near their calculated values, with coupling constants consistent with the presence of a Ph_2(H)P− unit (**1**, $J_{PH} = 456$ Hz; **2**, $J_{PH} = 470$ Hz). The ^{1}H NMR spectra of **1** and **2** each showed resonances arising from the six terminal BH's between 3.19 and −0.91 ppm, along with four intensity 1 resonances above −1.0 ppm that can be assigned to the three bridge-hydrogen resonances and one *endo*-CH resonance. The ^{1}H NMR spectrum of **1** also showed an intensity 2 resonance at 0.72 ppm arising from two *exo*-CH hydrogens, while that of **2** has, in addition to the

(11) (a) Williams, R. E. *Inorg. Chem.* **1971**, *10*, 210−214. (b) Rudolph, R. W.; Thompson, D. A. *Inorg. Chem.* **1974**, *13*, 2779−2782. (c) Wade, K. *Adv. Inorg. Chem. Radiochem.* **1976**, *18*, 1−66. (d) Williams, R. E. *Adv. Inorg. Chem. Radiochem.* **1976**, *18*, 67−142. (e) Williams, R. E. *Chem. Rev.* **1992**, *92*, 177−207.

(12) Jelínek, T.; Plesek, J.; Hermánek, S.; Stíbr, B. *Main Group Met. Chem.* **1987**, *10*, 397−398.

(13) (a) Kang, S. O.; Sneddon, L. G. *J. Am. Chem. Soc.* **1989**, *111*, 3281−3289. (b) Kang, S. O.; Sneddon, L. G. In *Electron Deficient Boron and Carbon Clusters*; Olah, G. A., Wade, K., Williams, R. E., Eds.; Wiley: New York, 1991; pp 195−213.

(14) Jelínek, T.; Stíbr, B.; Kennedy, J. D.; Hnyk, D.; Bühl, M.; Hofmann, M. *Dalton* **2003**, 1326−1331.

(15) Kadlecek, D. E.; Carroll, P. J.; Sneddon, L. G. *J. Am. Chem. Soc.* **2000**, *122*, 10868−10877.

Table 2. NMR Data[a,b,c]

compd	nucleus	δ (multiplicity, assignt, *J* (Hz))
endo-7-[Ph_2(H)P]-*hypho*-	^{11}B	−1.2 (br, B4), −3.3 (d, B6, J_{BH} > 119, overlapped), −25.9 (d, B5, J_{BH} 136), −29.3 (d, B2, J_{BH} > 128, overlapped), −30.5 (B3, overlapped), −56.5 (d, B1, J_{BH} 140)
7,8-$C_2B_6H_{12}$ (**1**)	^{11}B(calc)	−2.7 (B4), −5.4 (B6), −27.9 (B5), −32.2 (B2), −32.9 (B3), −62.5 (B1)
	^{1}H{^{11}B}	7.16−6.88 (m, phenyl), 5.58 (dd, P*H*, J_{PH} 454, J_{HH} 15), 3.87 (2, BH), 2.66 (1, BH), 2.22 (1, BH), 1.83 (1, BH), 0.72 (2, exo C*H*), 0.33 (1, BH), −1.16 (1, B*H*B), −1.90 (1, endo C*H*), −1.98 (1, B*H*B), −2.55 (d, B*H*B, J_{PH} 18)
	^{13}C	133.9−121.2 (phenyl, $J_{P9-C(phenyl)}$ 85 and 87[d]), −9.8 (t, C8, J_{CH} 155), −11.4 (br, C7, J_{CP} 66[d])
	^{13}C(calc)	138.6−130.0 (phenyl), −6.9 (C7), −8.0 (C8)
	^{31}P	19.0 (J_{PH} 456)
	^{31}P(calc)	30.8
endo-7-[Ph_2(H)P]-8-Me-	^{11}B	0.4 (br, B4), −4.5 (d, B6, J_{BH} 121), −27.3 (d, B5, J_{BH} ~152), −28.8 (d, B3, overlapped), −30.1 (d, B2, J_{BH} ~140), −58.1 (d, B1, J_{BH} 138)
hypho-7,8-$C_2B_6H_{11}$ (**2**)	^{11}B(calc)	−0.4 (B4), −5.5 (B6), −28.6 (B5), −30.4 (B3), −32.4 (B2), −63.2 (B1)
	^{1}H{^{11}B}	7.83−7.63 (m, phenyl), 6.23 (dd, P*H*, J_{PH} 467, J_{HH} 15), 3.19 (1, BH), 2.71 (1, BH), 1.75 (1, BH), 1.45 (1, BH), 1.24 (d, 3, CH_3, J_{HH} 6), 0.96 (qt, exo C*H*), 0.62 (1, BH), −0.91 (1, BH), −1.51 (1, B*H*B), −1.65 (1, endo C*H*), −2.22 (1, B*H*B), −2.79 (d, B*H*B, J_{HH} 16)
	^{13}C	134.7−121.3 (phenyl, $J_{P9-C(phenyl)}$ 85 and 87[d]), 20.2 (q, *C*H_3, J_{CH} 122), 0.6 (d, C8, J_{CH} 125), −11.5 (br, C7, J_{CP} 61[d])
	^{13}C(calc)	138.7−130.4 (phenyl), 21.7 (*C*H_3), 7.3 (C8), −7.1 (C7)
	^{31}P	21.4 (J_{PH} 470)
	^{31}P(calc)	32.5

[a] NMR shifts in ppm. [b] ^{1}H NMR at 500.4 MHz, ^{11}B NMR at 160.5 MHz, ^{13}C NMR at 125.8 MHz, and ^{31}P NMR at 145.8 MHz. [c] DFT/GIAO/NMR method (B3LYP/6-311G*// B3LYP/6-311G*). [d] Measured at −83 °C.

intensity 3 methyl resonance at 1.24 ppm, only an intensity 1 *exo*-CH resonance at 0.96 ppm. For both compounds, the P−H hydrogen resonance appeared as a doublet of doublets, **1** (5.58 ppm, J_{PH} = 454 Hz, J_{HH} = 15 Hz) and **2** (6.23 ppm, J_{PH} = 467 Hz, J_{HH} = 15 Hz), owing to its coupling to the phosphorus and the highest field bridge-hydrogen resonance. As expected, the ^{13}C NMR spectra of the compounds each gave two cage-carbon resonances near their calculated chemical shifts, with the *C*8-H_2 resonance in **1** appearing as a triplet and that of the Me-*C*8-H in **2** appearing as a doublet in their proton-coupled spectra. At room temperature, the phosphorus-substituted C7 resonance in both compounds was broad, owing to coupling with both boron and phosphorus. When the spectra were recorded at −83 °C, the ^{13}C−^{11}B coupling at C7 was thermally decoupled[16] and each resonance appeared as a sharp doublet with the magnitude of the observed coupling (J_{P9-C7} = 66 Hz (**1**), 61 Hz (**2**)) being smaller than that found for the two phenyl carbons bonded to P9 ($J_{P9-C(phenyl)}$ = 85 and 87 Hz (**1**), 85 and 87 Hz (**2**)).

While the structure of *hypho*-$C_2B_6H_{13}^-$ has not been crystallographically determined, **1** and **2** can be compared with the structures of the isoelectronic eight-vertex 2,3-Me_2-*hypho*-2,3-$S_2B_6H_8$.[13] In 2,3-Me_2-*hypho*-2,3-$S_2B_6H_8$, the Me−S groups adopt the bridging positions that are occupied by the C7 and C8 carbons in **1** and **2** on the basal pentagonal plane of the boron fragment. In both **1** and **2**, the dihedral angles formed by the basal B2,3,4,5,6 pentagonal plane with the two C7−B2−B6 and C8−B3−B4 planes are similar (120.3°, 120.9°, **1**; 120.2°, 120.6°, **2**) but are inclined greater with respect to the basal plane than the equivalent S−B−B planes in 2,3-Me_2-*hypho*-2,3-$S_2B_6H_8$ (109°), thus yielding structures more open than that of 2,3-Me_2-*hypho*-2,3-$S_2B_6H_8$.

Of most interest, it was found that the P9−C7 bond distances in **1** (1.737(3) Å) and **2** (1.742(3) Å) are significantly shortened compared to the P9−C10 and P9−C16 (1.781(3) and 1.801(3) Å, **1**; 1.797(3) and 1.795(3) Å, **2**) distances. These differences are also consistent with the differences in the DFT calculated values of P9−C7 (1.747 Å, **I**; 1.748 Å, **II**) versus the P9−C10 and P9−C16 bond distances (1.823 and 1.815 Å, **I**; 1.824 and 1.815 Å, **II**) in the DFT optimized structures of **I** and **II**. The P9−C7 distances, in fact, fall into the range found in substituted phosphorus ylides, suggesting some double-bond character in the P9−C7 bonds.[17] Population analysis calculations[18] for **I** and **II** also established that, as in phosphorus ylides, P9 and C7 have strong positive and negative charges, respectively (Table 3).

As shown in the examples below, a number of borane adducts of phosphorus ylides[19] (eqs 2−5) and C-borylated substituted phosphorus ylides[20] (eq 6) have been previously synthesized and structurally characterized.

$$2R_3P{=}CH_2 + B_2H_6 \rightarrow 2R_3P^+{-}CH_2BH_3^- \quad (2)$$

$$R_3P{=}CPhH + B(C_6F_5)_3 \rightarrow R_3P^+{-}CPhH{-}B(C_6F_5)_3^- \quad (3)$$

$$R_3P{=}CH_2 + B_3H_7THF \rightarrow R_3P^+{-}CH_2^+{-}B_3H_7^- + THF \quad (4)$$

$$R_3P{=}CH_2 + \textit{closo}\text{-}2,3\text{-}Et_2C_2B_5H_5 \rightarrow 6\text{-}(R_3P^+\text{-}CH_2)\text{-}3,4\textit{-nido}\text{-}3,4\text{-}Et_2C_2B_5H_5^- \quad (5)$$

$$(R_2N)_2P{=}C{-}SiMe_3 + R'_2BF \rightarrow (R_2N)_2(F)P{=}C(BR'_2)(SiMe_3) \quad (6)$$

In the phosphorus ylide borane adducts, the P−C bond distances range from 1.756 to 1.795 Å, while the substituted ylide in eq 6 exhibits a much shorter P−C

(16) (a) Wrackmeyer, B. In *Progress in NMR Spectroscopy*; Emsley, J. W., Feeney, J., Sutcliffe, L. H., Eds.; Pergamon: New York, 1979; Vol. 12, pp 227−259. (b) Gragg, B. R.; Layton, W. J.; Niedenzu, K. *J. Organomet. Chem.* **1977**, *132*, 29−36.

(17) For example, see: (a) Schmidbaur, H.; Jeong, J.; Schier, A.; Graf, W.; Wilkinson, D. L.; Müller, G., Krüger, C. *New J. Chem.* **1989**, *13*, 341−352. (b) Ammon, H. L.; Wheeler, G. L.; Watts, P. H., Jr. *J. Am. Chem. Soc.* **1973**, *95*, 6158−6163. (c) Speziale, A. J.; Ratts, K. W. *J. Am. Chem. Soc.* **1965**, *87*, 5603−5606. (d) Bestmann, H. J.; Furst, T. G.; Schier, A. *Angew. Chem., Int. Ed. Engl.* **1993**, *32*, 1746−1747.

(18) Glendening, E. D.; Reed, A. E.; Carpenter, J. E.; Weinhold, F. NBO Version 3.1. The calculations were done at the B3LYP/6-311G* level.

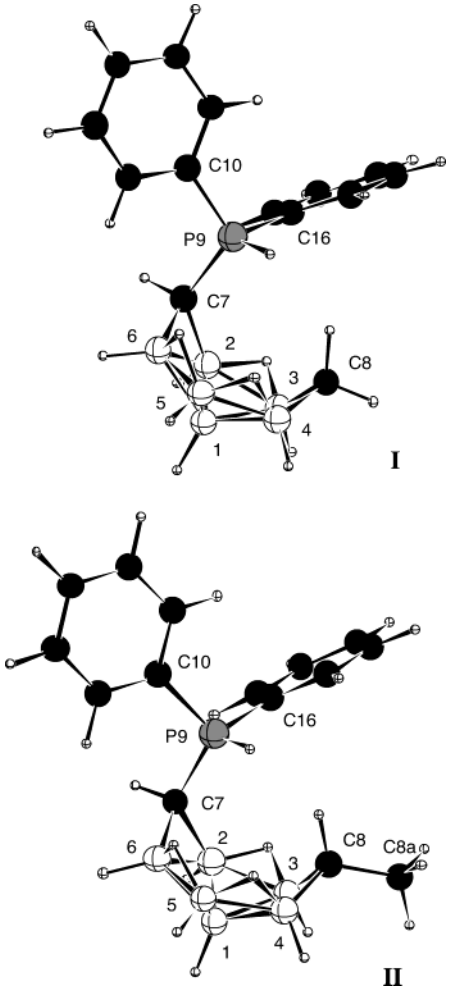

Figure 3. Optimized geometries of **I** and **II** (**1** and **2**, B3LYP/6-311G*). Selected calculated bond distances (Å) and angles (deg) are as follows. **I**: P9−C7, 1.747; P9−C10, 1.823; P9−C16, 1.815; P9−H9, 1.406; B2−C7, 1.636; B6−C7, 1.627; B3−C8, 1.598; B4−C8, 1.577; B2−B6, 2.006; B2−B3, 1.813; B3−B4, 1.998; B4−B5, 1.801; B5−B6, 1.796; C7−P9−C10, 111.1; C7−P9−C16, 116.3; C10−P9−C16, 108.6; C7−P9−H9, 111.1; P9−C7−C7H, 107.0; C8Ha-C8−C8Hb, 109.1. **II**: P9−C7, 1.747; P9−C10, 1.824; P9−C16, 1.815; P9−H9, 1.405; B2−C7, 1.635; B6−C7, 1.629; B3−C8, 1.600; B4−C8, 1.580; B2−B6, 2.004; B2−B3, 1.813; B3−B4, 1.989; B4−B5, 1.803; B5−B6, 1.796; C7−P9−C10, 110.9; C7−P9−C16, 116.6; C10−P9−C16, 108.5; C7−P9−H9, 111.2; C8a−C8−C8H, 110.4; P9−C7−C7H, 106.9.

Table 3. Natural Population Analysis (Natural Charge) at the B3LYP/6-311G* Level

	I	II	A	B	C
P9	1.407	1.407	1.359	1.363	1.414
C7	−1.087	−1.087	−0.939	−1.170	−1.047
C10	−0.361	−0.361	−0.364	−0.356	−0.370
C16	−0.368	−0.368	−0.358	−0.357	−0.361
C8	−0.900	−0.715			

bond length of 1.696(2) Å. The P9−C7 bond distances found for **1** and **2** lie between the values found for the ylide borane adducts and the C-borylated ylide.

(19) (a) Schmidbaur, H.; Müller, G.; Milewski-Mahrla, B.; Schubert, U. *Chem. Ber.* **1980**, *113*, 2575−2578. (b) Döring, S.; Erker, G.; Fröhlich, R.; Meyer, O.; Bergander, K. *Organometallics* **1998**, *17*, 2183−2187. (c) Andrews, S. J.; Welch, A. J. *Acta Crystallogr.* **1985**, *C41*, 1496−1499. (d) Su, K.; Fazen, P. J.; Carroll, P. J.; Sneddon, L. G. *Organometallics* **1992**, *11*, 2715−2718.

(20) Locquenghien, K. H. v.; Baceiredo, A.; Boese, R.; Bertrand, G. *J. Am. Chem. Soc.* **1991**, *113*, 5062−5063.

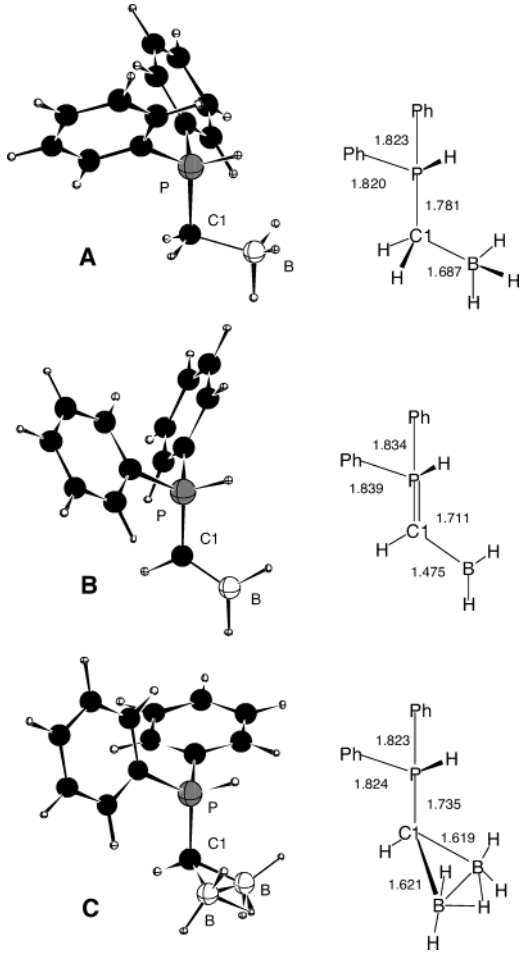

Figure 4. Optimized geometries and selected bond lengths for $Ph_2(H)P-CH_2-BH_3$ (**A**), $Ph_2(H)P=C(H)-BH_2$ (**B**), and $Ph_2(H)P-C(H)-B_2H_5$ (**C**).

The nature of the P−C bonding in **1** and **2** was further explored computationally using the model compounds $Ph_2(H)P-CH_2-BH_3$ (**A**), $Ph_2(H)P=C(H)-BH_2$ (**B**), and $Ph_2(H)P-C(H)-B_2H_5$ (**C**). DFT calculations yielded the optimized structures shown in Figure 4. Structure **A** provides a model for an ylide−borane adduct, while structure **B** can be used to model a C-borylated substituted ylide. In one limit, the P−C1 and C1−B bonds in the ylide−borane adduct **A** are dative bonds involving the donation of a lone pair of electrons from P to C1 and from C1 to BH_3, whereas the C1−B bond in the boron-substituted ylide **B** is a two-center, two-electron bond where C1 and B each contribute one electron and P−C1 is a formal double bond. Consistent with this interpretation and the crystallographically determined bond distances discussed above, the calculated P−C1 distance in the ylide−borane adduct **A** (1.781 Å) is significantly longer than that in the substituted ylide **B** (1.711 Å).

In structure **C**, as in **1** and **2**, the carbon bridges a B−B bond. As shown in Figure 5, the bonding in **C** can be viewed in two different ways: (1) in structure **Ca**, the C1 carbon can be viewed as donating one electron and only one orbital to the B_2H_5 unit, forming a three-center, two-electron bond, with P−C1 having multiple-bond character; (2) in resonance structures **Cb** and **Cb′**, the C1 carbon could be viewed as donating three electrons to the B_2H_5 unit by forming a two-center, two-electron bond with one boron and a dative two-electron

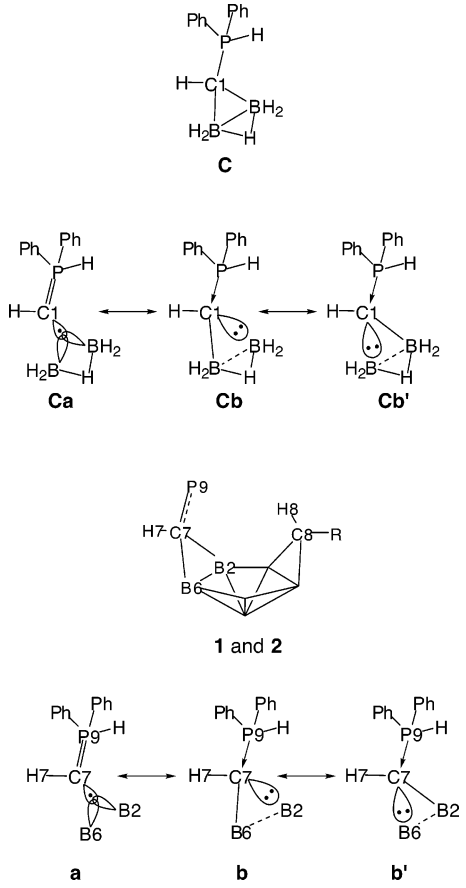

Figure 5. Limiting bonding descriptions in $Ph_2(H)P-C(H)-B_2H_5$ (**C**) and *endo*-7-[$Ph_2(H)P$]-8-R-*hypho*-7,8-$C_2B_6H_{11}$ (**1** and **2**).

bond with the other boron. In (2), the P−C1 bond would be considered a dative bond with a lone electron pair on P being donated to C1 as in structure **A**. Obviously, **Ca** and **Cb**/**Cb′** are limiting bonding descriptions, and the bonding in **C** is probably a mixture of both components; indeed, the P−C1 distance calculated for **C** (1.735 Å) is between the values calculated for structures **A** and **B** in Figure 4.

Structure **C** is analogous to that of the P9−C7−B2−B6 fragment in **1** and **2**, with the calculated P−C1 distance of 1.735 Å being nearly identical with the P9−C7 distances measured for **1** and **2** and calculated for structures **I** and **II**. The C7−B2 and C7−B6 distances are also close to the calculated values for C1−B distances for **C** (1.619 and 1.621 Å). Population analysis calculations for **A**−**C** showed that **C** has, in fact, a charge distribution pattern similar to those of **1** and **2** (Table 3). As was the case for **C**, two limiting cases can be described for the P9−C7 bonding in **1** and **2**: (1) in structure **a** in Figure 5, the C7 carbon donates one orbital and one electron to the B2−B6 edge, forming a three-center, two-electron bond, with P−C7 having ylide-like multiple-bond character; (2) as shown in resonance structures **b** and **b′**, C7 donates three electrons to the cage system, forming a two-center, two-electron bond at one boron and a dative two-electron bond at the other.

Again, the actual bonding in **1** and **2** is undoubtedly a mixture of both **a** and **b**/**b**, but the shortened P−C1 bond length suggests that **a** may make a substantial contribution. If this were in fact the case, then, as shown

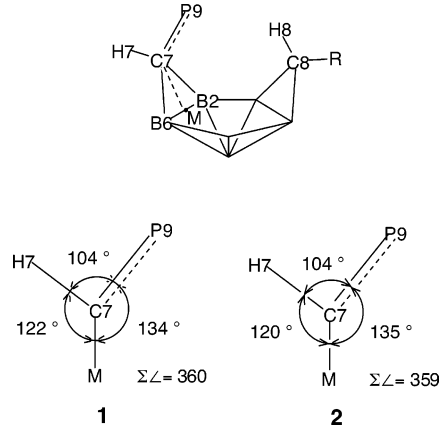

Figure 6. Calculated bond angles at the C7 carbons in *endo*-7-[$Ph_2(H)P$]-8-R-*hypho*-7,8-$C_2B_6H_{11}$ (**1** and **2**).

in Figure 6, the C7 orbital would be directed toward the midpoint (M) of the B2−B6 edge. The P9−C7−M, P9−C7−H7, and H7−C7−M angles were calculated to be 134, 104, and 122° in **1** and 135, 104, and 120° in **2**, respectively, summing in both cases to ∼360°. Thus, C7, H7, P9, and M are planar, and C7 could then utilize approximately sp^2 type hybrid orbitals to form both a σ bond with H7 and a dative bond with a lone pair of electrons on P9, while donating one other lobe and one electron to form a three-center, two-electron bond with B2 and B6. This would then leave an electron pair in the p orbital on C7 that is orthogonal to the sp^2 orbitals to form a π-bonding interaction with P9. Such multiple-bond character in the P9−C7 bond in **1** and **2** might also be expected to weaken the bonding interaction of C7 with B2 and B6, and in fact, the C7−B2 and C7−B6 distances (1.612(5) and 1.618(5) Å, **1**; 1.624(4) and 1.620(4) Å, **2**) are slightly longer than the C8−B3 and C8−B4 distances (1.603(6) and 1.570(6) Å, **1**; 1.587(4) and 1.565(4) Å, **2**).

From a cluster-electron-counting point of view, the **1** and **2** cage structures can also be viewed in two different ways. As discussed earlier, if both cage carbons are considered to be parts of the cage framework, then **1** and **2** would be eight-vertex hypho clusters with exopolyhedral $Ph_2(H)P-$ substituents: i.e., *endo*-7-[Ph_2-(H)P]-8-R-*hypho*-7,8-$C_2B_6H_{11}$. On the other hand, if the $Ph_2P(H)=C(H)-$ unit is considered to be a carborane-substituted phosphorus ylide (i.e. similar to structure **B** in Figure 4) that is bonded to the cage B2−B6 edge, then **1** and **2** can be viewed as seven-vertex arachno clusters, $\mu_{2,6}$-[$Ph_2(H)P=C(H)$]-8-R-*arachno*-8-CB_6H_{10}. The CB_6 cage structures in **1** and **2** are, in fact, quite similar to the *arachno*-$B_7H_{12}^-$ borane fragment found in the $Fe(CO)_4B_7H_{12}^-$ complex,[21] supporting the $\mu_{2,6}$-[$Ph_2(H)P=C(H)$]-8-R-*arachno*-8-CB_6H_{10} formulation.

In summary, the experimental and computational results presented above indicate that the bonds between the phosphorus and cage carbons in the phosphine-substituted carboranes **1** and **2** have an ylide-like multiple-bond character. While both phosphorus ylide borane adducts and C-borylated, substituted phosphorus ylides were previously known, **1** and **2** are unique in that they have the first examples of ylidic carbons

(21) Mangion, M.; Clayton, W. R.; Hollander, O.; Shore, S. G. *Inorg. Chem.* **1977**, *16*, 2110−2114.

that can also be considered as a part of a cluster framework.

Acknowledgment. We thank the National Science Foundation for the support of this research.

Supporting Information Available: Tables giving Cartesian coordinates for DFT optimized geometries and X-ray crystallographic data for structure determinations of compounds **1** and **2** as CIF files. This material is available free of charge via the Internet at http://pubs.acs.org.

OM034274H